



# Water and Sand Inrush During Mining Under Thick Unconsolidated Layers and Thin Bedrock in the Zhaogu No. 1 Coal Mine, China

Yanchun Xu<sup>1</sup> · Yaqi Luo<sup>1</sup> · Jianghua Li<sup>2</sup> · Kunqi Li<sup>1</sup> · Xuchu Cao<sup>1</sup>

Received: 26 March 2017 / Accepted: 29 March 2018 / Published online: 4 April 2018  
© Springer-Verlag GmbH Germany, part of Springer Nature 2018

## Abstract

Raising the upper boundary of coal mining under thick Cenozoic unconsolidated layers has brought new challenges to the prediction and prevention of water and sand inrush from overlying sand and gravel aquifers in north China. The mechanism of water and sand inrush was studied based on an incident that occurred at working face 11071 in the Zhaogu No. 1 coal mine, in Henan Province. Geological and hydrogeological investigations in overlying strata indicated that intersections of horizontal confined aquifers and inclined bedrock surfaces, defined as skylight areas, allow water and sand from the aquifers to enter the workings. Geotechnical and physical simulation tests on overlying strata showed that mining-induced fractures in weathered bedrock were gradually enhanced by water and sand flowing under high pressure, leading to inrush incidents at the working faces. The empirical formula for estimating the requisite size of coal and rock pillars were modified by incorporating a term for protective thickness under skylight areas. The modified formula was successfully applied to the extraction of neighboring faces, proving its applicability in coal mines with similar geological and hydrogeological conditions.

**Keywords** Coal mining · Water hazard · Skylight areas · Fracture evolution in mudstone · Coal and rock pillars

## Introduction and Background

In northern China, sand and gravel aquifers at the bottom of thick, unconsolidated Cenozoic layers are potential mine water hazards during coal exploitation under bedrock surfaces (Chen et al. 2014; Zhang and Shen 2004; Zhou et al. 2016). With exhaustion of shallow coal resources and an urgent demand for an increased rate of coal recovery, the upper boundary of coal mining in the region has been raised in recent years (Sun et al. 2008; Zhang et al. 2011). However, this has greatly increased the likelihood of water and sand inrush, especially in thin-bedrock areas, due to the shortened distance from the mine workings to the aquifers (Yang et al. 2011; Zhang et al. 2016).

Much research has been carried out to understand the mechanisms of water and sand inrush in workings under

unconsolidated layers (Miao et al. 2011; Shi et al. 2017; Wu et al. 2015; Zhang et al. 2009, 2015). It is widely acknowledged that once mining-induced fractures extend upward into confined aquifers, these fractures can serve as passageways between aquifers and workings, triggering water and sand inrush (Bai and Elsworth 1990; Zhang et al. 2017). The height of the water-conducting fractured zone is highly related to mining conditions and the lithology of the overlying strata, and empirical formulae for height estimation were given based on numerous in situ observations (State Bureau of Coal Industry 2000; Tan et al. 2017). Compound breakage of key strata caused by load transfer of an unconsolidated confined aquifer was proposed as an additional reason for water and sand inrush based on numerical simulation and field experiments (Wang et al. 2012; Xu et al. 2011). The scale of water and sand inrush was primarily decided by the initial water pressure in the confined aquifers and the hydraulic conductivity of the mining-induced fractures (Chen et al. 2017; Yao et al. 2012).

Retaining protective coal and rock pillars above working faces proved to be an effective way to prevent water and sand inrush. The sizes of pillars under different geological and hydrogeological conditions are usually decided by empirical formulae (Zhang and Peng 2005). Dewatering and

✉ Yaqi Luo  
yaqi.luo@hotmail.com

<sup>1</sup> School of Resources and Safety Engineering, China University of Mining and Technology, Beijing 100083, China

<sup>2</sup> Mine Safety Technology Branch, China Coal Research Institute, Beijing 100013, China

drainage of overlying confined aquifers also helped prevent water and sand inrush by lowering water pressure prior to coal extraction (Yang et al. 2011; Zhang et al. 2013b). A clay layer between the lowermost sand and gravel aquifer and the bedrock was regarded as a protective layer because the clay expands in volume when mixed with water, inhibiting expansion of the mining-induced fractures (Huang et al. 2010; Xu 2008).

Most studies on water and sand inrush in thin-bedrock areas under thick, unconsolidated layers have focused on places where a lower unconsolidated layer was deposited parallel to the bedrock surface. In this study, we investigated the mechanism of water and sand inrush at working face 11071 in the Zhaogu No. 1 coal mine where a horizontal aquifer with low water abundance extended and intersected an inclined bedrock surface. An impervious clay layer beneath the lowermost unconsolidated aquifer hindered water drainage to the neighboring working faces, which increased water pressure in the aquifer. Mining-induced fractures in direct contact with the confined aquifer gradually increased in size, which led to water and sand inrush. To ensure safety in this special geological condition, the size of the protective pillars was modified.

### Risk Analysis of Water and Sand Inrush in Thin-Bedrock Areas

On 7th July 2011, water and sand inrush occurred at working face 11071 during the first weighting of the main roof. Water kept flowing from above, with the rate increasing for more than 30 h before it finally stopped. The maximum water inflow reached 120 m<sup>3</sup>/h, and 3000 m<sup>3</sup> of mud and sand accumulated at the working face and the entries. To prevent the re-occurrence of such an event and to ensure safety at subsequent faces, the risk of a potential inrush was evaluated.

### Geological and Hydrogeological Conditions in Thin-Bedrock Areas

The thickness of different geologic layers from the ground surface to coal seam II<sub>1</sub> were estimated from core samples of 13 boreholes located all over the Zhaogu Mine, from the surface to a few meters below seam II<sub>1</sub>. The thickness of the seam ranged from 3.9 to 6.9 m, averaging 6.1 m. The average thickness of the coal seam at working face 11071, where the two slice-mining method was used, was 6.1 m. The top slice was 3.3 to 3.5 m thick, and the remaining thickness corresponded to the second slice. The thickness of the Cenozoic unconsolidated layers was 453 m, on average, and several sand and gravel layers of varying thickness from 2.2 to 14.0 m existed near the bottom of the unconsolidated

layers. A clay layer, ranging from 5.7 to 63.8 m in thickness, 34.5 m on average, was directly below the lowermost sand and gravel layer. The bedrock in the roof of seam II<sub>1</sub> was categorized as moderately hard rock, and its thickness ranged from 13.9 to 95.5 m, averaging 44.8 m. The cross-section from the surface to the coal seam in a thin-bedrock area (Fig. 1), was estimated based on the borehole data.

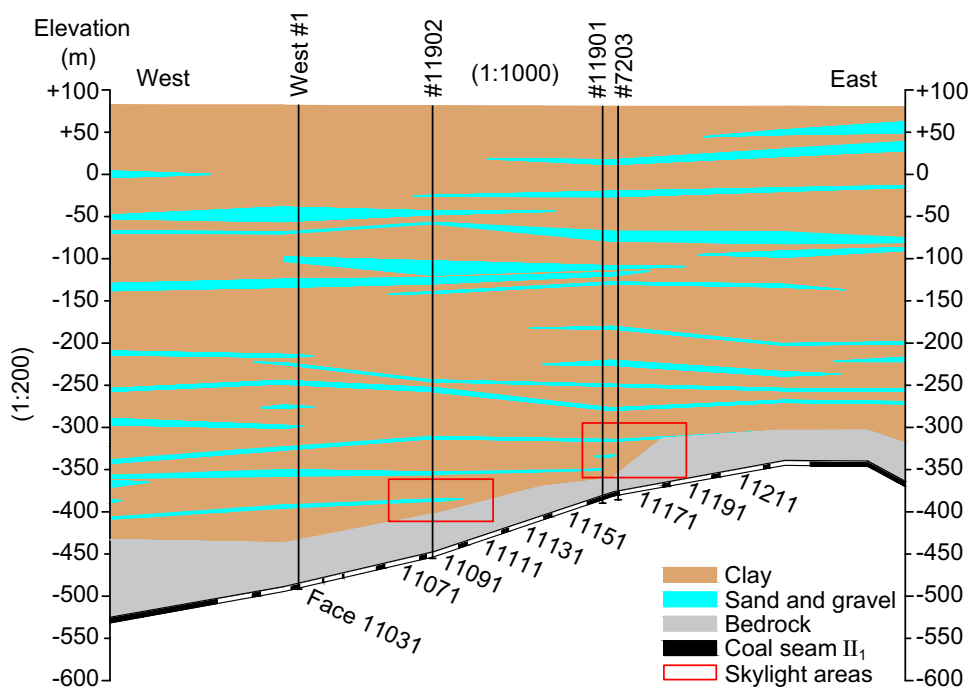
The unconsolidated layers, which mainly consisted of clay and sandy clay, were interbedded with multiple sand and gravel aquifers (Fig. 1). The total thickness of the unconsolidated layers ranged from 380 to 520 m and generally increased from east to west. Three sand and gravel aquifers, separated by thick clay layers, existed at the bottom of the unconsolidated layers. The sand and gravel aquifers, deposited horizontally, extended and intersected or approached the inclined bedrock surface, forming skylight areas (Fig. 1). Water and sand inrush was more likely to occur under the skylight areas where the protective effect of the clay layer was greatly weakened. A similar inrush accident occurred at working face 7172 in the Xuzhuang coal mine where a skylight area was formed where part of the bedrock surface was uplifted and intersected a sand and gravel aquifer at the bottom of the unconsolidated layers, indicating the importance of this study on water and sand inrush for this unusual condition.

### Risk Zoning for Potential Water and Sand Inrush

To predict spots of potential mining-induced water and sand inrush, 686 exploration boreholes were drilled in the roof along the entries of six working faces (faces 11111, 11131, 11151, 11171, 11191, and 11211). Water discharging from these boreholes was mostly less than 5 m<sup>3</sup>/h with no flowing sand, whereas sand discharges were observed under poorly consolidated clay. Areas of potential water and sand inrush were plotted in grey shadows (Fig. 2a, b) using Surfer (Golden Software, USA), based on the amount of sand and water discharging from the boreholes. Isopach maps of the bedrock and the unconsolidated layers in the study area (Fig. 2a, b, respectively) were used to investigate the relationship of potential inrush and the thickness of the overburden strata.

The shadowed areas in Fig. 2a fell on the contour lines of a wide range of thickness, from 32 to 52 m, and no relationship was found between the potential inrush spots and the thickness of the bedrock. However, the shadowed areas in Fig. 2b fell in two bands, between 390 and 420 m and between 460 and 470 m, which corresponded to the skylight areas in Fig. 1, indicating that the potential inrush spots were related to the thickness of the unconsolidated layers. To better understand the geological and hydrogeological conditions at these depths, partial stratigraphic columns of four observation boreholes (boreholes 7203 and 11901 in the east

**Fig. 1** Cross-section from the ground surface to coal seam II<sub>1</sub> in a thin-bedrock area



coalfield and 11902 and west No. 1 in the west coalfield, see Fig. 1) are shown in Fig. 3. One or two thin sand and gravel aquifers, sources of water and sand in the roof boreholes, were found within each band. The aquifer in Fig. 3b is confined by impervious clay layers and might be the water and sand source of the inrush incident that occurred at working face 11071.

Preliminary analysis indicated that water and sand inrush was more likely at working faces under the skylight areas where the lowermost horizontal confined aquifers in the unconsolidated layers extended and intersected the inclined bedrock surface or where the thickness of the lowermost clay layer became too thin. Without the protection of the lowermost impermeable clay layer, aquifers in direct contact with the bedrock posed threats to mine safety during extraction of the underlying coal.

### Mechanism of Water and Sand Inrush in the Thin-Bedrock Area

Water pressure in the lowermost unconsolidated aquifers and the evolution of mining-induced fractures in shallow bedrock were the two aspects that were most closely related to water and sand inrush. To investigate the mechanism of the inrush that occurred at working face 11071, the water resistance of clay and mudstone samples from under the lowermost aquifer in the west coalfield was tested, and fracture evolution in the mudstone was modeled in physical simulation tests.

### Geological Model of Mining-Induced Water and Sand Inrush

According to the preliminary analysis, the aquifer under the skylight areas was the main water source of the water and sand inrush incident. Two failure zones, also referred to as the “Two Zones”, were formed in the overlying strata during mining: a caving zone and a fractured zone (Bai and Elsworth 1990; Liu et al. 2015). Fractures in the fractured zone could be a trigger for the failure in the overlying strata. A simplified geological model for mining-induced water and sand inrush under a skylight area was established (Fig. 4). In most cases, water pressure in the aquifers would decrease during extraction of adjacent faces by water draining through mining-induced fractures, which would help prevent water and sand inrush at the mining faces under the skylight areas. However, the inrush at working face 11071 indicated that the underlying clay layer hindered such drainage, thus maintaining high pressure in the lowermost sand and gravel aquifer.

### Water Resistance of the Lowermost Clay Layer

Clay at the bottom of the unconsolidated layers played an important role in preventing water and sand inrush from the overlying sand and gravel aquifers by inhibiting fractures from enlarging (Huang et al. 2010). Its water resistance was inferred through liquid and plastic limit tests. To this end, five soil samples ( $S_1$ – $S_5$ ) were collected at different depths between 470 and 520 m from core samples of two roof boreholes that had been used to observe the height of the “Two

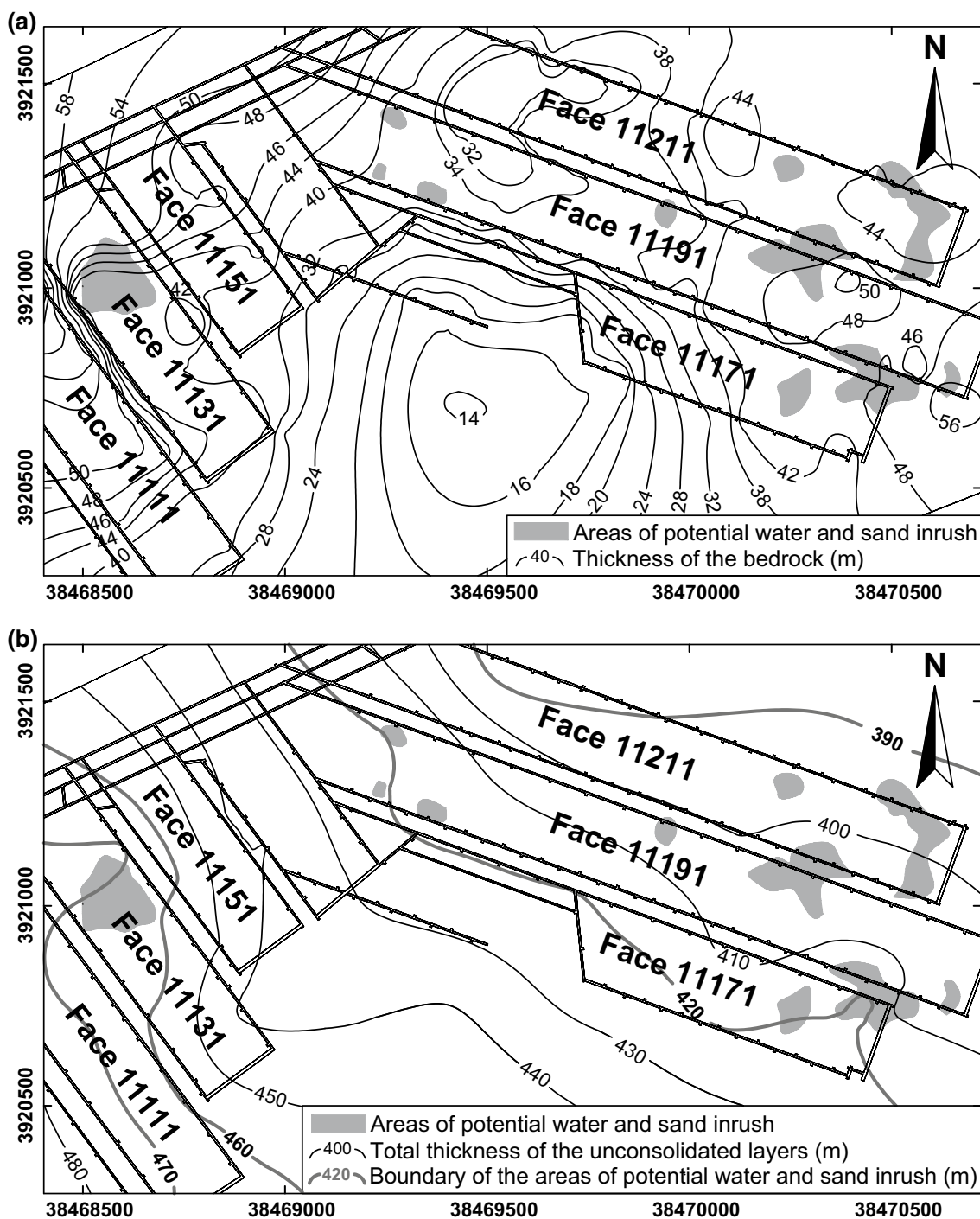
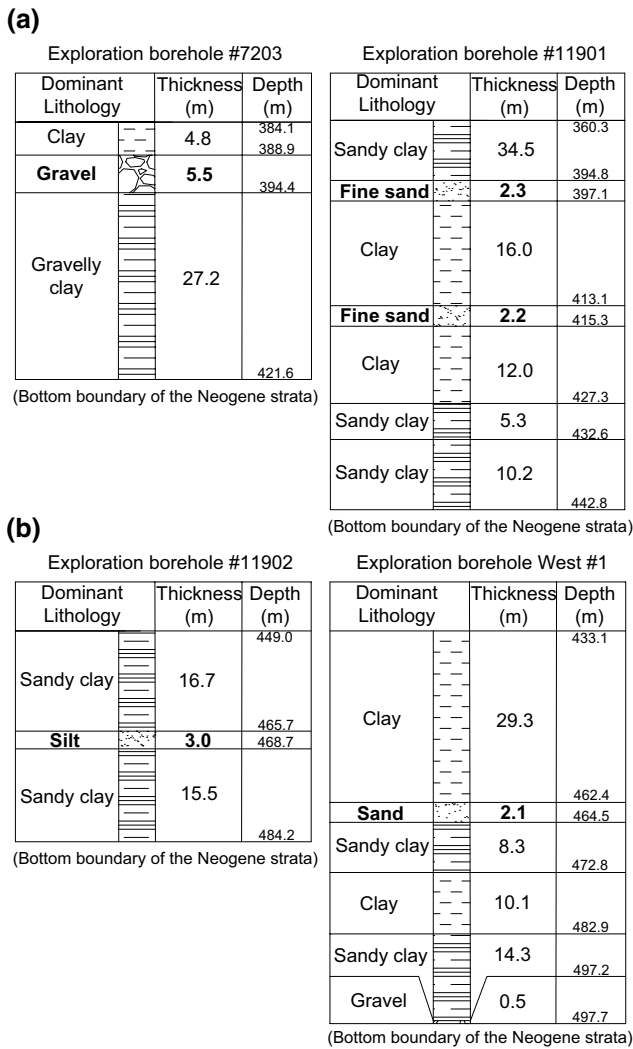


Fig. 2 Areas of potential water and sand inrush and isopach maps of a the bedrock and b the unconsolidated layers

Zones” in overlying strata near working face 11071. The results of laboratory tests with a GYS-2 photoelectric liquid and plastic limit tester (Nanjing Soil Instrument Factory Co., Ltd., China) are shown in Table 1.

All five soil samples had plasticity indices greater than 10, and three of the indices exceeded 17 (Table 1). Soil with a plasticity index greater than 10 or 17 was considered

to be clay with fair or good water resistance, respectively. The liquidity indices were all less than 0, indicating that the soil samples were in a semi-consolidated state with poor fluidity. It was therefore concluded that the lowermost clay layer had good water resistance and poor fluidity, which was favorable for preventing an inrush from an overlying aquifer. However, these advantages hindered



**Fig. 3** Partial stratigraphic columns of the lowermost aquifers in the unconsolidated layers **a** in the east coalfield and **b** in the west coalfield

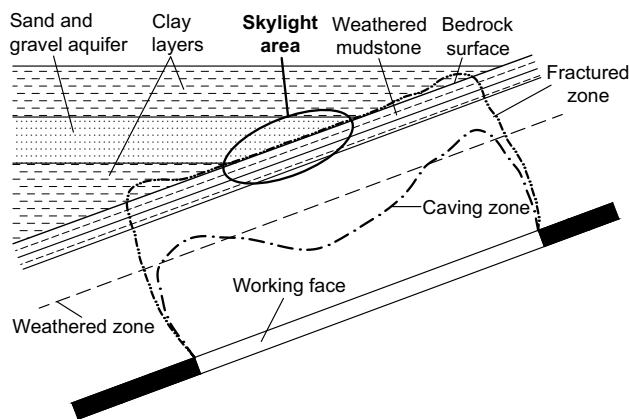


**Fig. 4** Geological model for mining-induced water and sand inrush under a skylight area

drainage to adjacent working faces, thus increasing water pressure in the overlying aquifer.

### Weathering of Shallow Bedrock

Shallow bedrock in an outcrop area undergoes different degrees of weathering, resulting in varied physical and engineering properties at different depths. Weathered mudstone was greatly softened and tended to heal interior fractures as water flowed through the fractures under low water pressure. In other words, weathering lowered the strength of mudstone but enhanced its water resistance. In contrast, weathered sandstone developed more fractures, which reduced its block size and increased its water abundance. Therefore, characterization of bedrock lithology and a reasonable division of weathered and unweathered zones are required to ensure safety under water bodies.

### Point Load Test for Shallow Bedrock

For a specific mining area, it is reasonable to divide weathered and unweathered zones based on the rocks' lithological characteristics and strength. For this study, a point load test were used to divide weathered and unweathered zones in shallow bedrock, based on the Standard for Engineering Classification of Rock Mass in China (GB 50218-1994). Two groups of rock samples were collected at different intervals along the core samples of two roof boreholes drilled in the crosscut of face 11171 (Group A) and in the headgate of face 11191 (Group B). The description of the core samples indicated that mudstone and sandstone were alternatively deposited in the shallow bedrock. Due to the distinctive ranges of point load strength for mudstone and sandstone, only one kind of rock was used for the test. The point load strength index ( $I_{s(50)}$ ) of the six mudstone samples in Group A and four mudstone samples in Group B at different depths was measured with an SD-1 digital point load tester (Beijing Zhongke Dongchen Technology Co., Ltd., China) and was plotted with respect to distance from the bottom of the unconsolidated layers.

As shown in Fig. 5, the  $I_{s(50)}$  was 0 in the first 10 m under the unconsolidated layers for Group A and in the first 5 m for Group B, which indicated a strong weathering effect and weak cohesive forces between rock particles in these zones. Between 10 and 14.5 m under the unconsolidated layers for Group A and between 5 and 14.5 m for Group B,  $I_{s(50)}$  increased dramatically due to the mitigated weathering effect with depth. The  $I_{s(50)}$  of mudstone more than 14.5 m from the unconsolidated layers was relatively stable, which indicated minor weathering in this zone. Hence, the dividing line between the weathered and unweathered zones in shallow bedrock was estimated to be 14.5 m under the unconsolidated layers (see the dashed line in Fig. 5).

**Table 1** Results of liquid and plastic limit tests for soil samples from overlying strata near working face 11071

Soil sample	Depth (m)	Liquid limit (%)	Plastic limit (%)	Plasticity index (%)	Soil classification	Liquidity index	State of soil
S <sub>1</sub>	478.1–482.2	38.0	15.0	23.0	Low liquid limit clay	−0.15	Hard
S <sub>2</sub>	483.3–484.9	31.0	15.2	15.8	Low liquid limit clay	−0.23	Hard
S <sub>3</sub>	478.5–485.4	27.4	15.4	12.0	Low liquid limit clay	−0.15	Hard
S <sub>4</sub>	497.5–499.8	32.4	13.6	18.8	Low liquid limit clay	−0.18	Hard
S <sub>5</sub>	515.8–516.7	31.2	12.6	18.6	Low liquid limit clay	−0.10	Hard

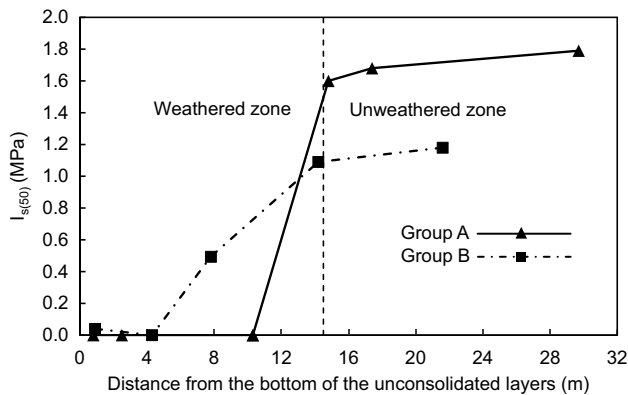


**Fig. 5** The point load strength index ( $I_{s(50)}$ ) of mudstone samples in shallow bedrock

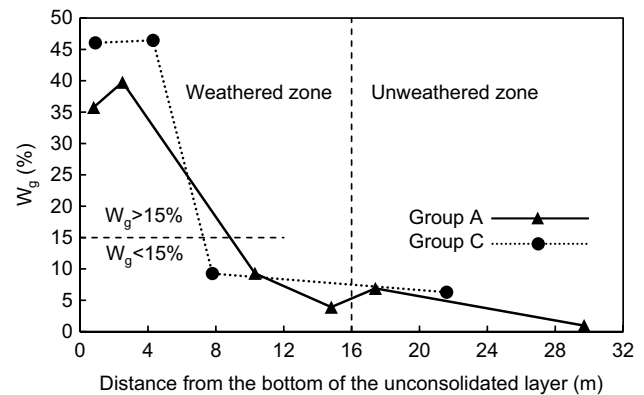


**Fig. 6** Dry-saturated water absorption ( $W_g$ ) of mudstone samples in shallow bedrock

**Dry-Saturated Water Absorption Test**

Weathering weakened the particle connectivity, decomposed the primary minerals, and resulted in fractures and secondary clay minerals in the shallow bedrock. The dry-saturated water absorption ( $W_g$ ), defined as the ratio of the maximum water absorption of a rock to its solid mass, is widely used as an indication of particle connectivity and the hydrophilic property of the mineral composition (State Administration of Work Safety 2009). In other words, the  $W_g$  of a rock reflects both its water resistance and degree of weathering.

Another group of rock samples (Group C) were collected from the core sample of a roof borehole drilled in the tailgate of face 11171. The dry-saturated water absorption test was performed for six mudstone samples in Group A and four mudstone samples in Group C. According to the Standard for Test Methods of Engineering Rock Mass in China (GB/T 50266-2013), the rock samples were thoroughly dried in a GZX-9076MBE Electric Blast drying oven (Shanghai Boxun Industry & Commerce Co., Ltd., China) at a temperature between 105 and 110 °C for 24 h and were then forcibly saturated in boiling water for more than 6 h. The  $W_g$  of the rock samples was calculated and plotted with respect to distance from the bottom of the unconsolidated layers (Fig. 6).

A continuous decline of the  $W_g$ —distance curve indicates that the shallow bedrock was more weathered than

the deeper bedrock. The degree of weathering at different depths was inferred from the slope change of each curve.  $W_g$  reached its highest value in the first 5 m before sharply decreasing in the following 5 m, and then stabilizing from 10 m under the bedrock surface for Group A and from 8 m for Group C. The  $W_g$  of the unweathered mudstone was below 6% (Qu et al. 1988; Zhang et al. 2013a), so the boundary of the weathered and unweathered zones was estimated to be  $\approx$  16 m below the bedrock surface (see the vertical dashed line in Fig. 6). On the other hand, rock with a  $W_g$  greater than 15% has good water resistance (State Administration of Work Safety 2009). The  $W_g$  values within 7 m of the bedrock surface all exceeded 15%, and some even reached 35% within the first 4 m (see the horizontal dashed line in Fig. 6).

Data from the dry-saturated water absorption test indicated that the weathered zone extended to a depth of 16 m below the bedrock surface, and that the clay in the first 4 m had good water resistance. This result was close to that in the point load test, so the mudstone in the shallow bedrock was considered to be effective in preventing water and sand inrush from overlying aquifers with low water pressure.

## Physical Simulation Tests of the Failure Process in Mudstone

The unpredictability of water and sand inrush made it difficult to observe the failure process by making in situ measurements in mudstone. Therefore, a scaled model was built to understand the mechanism of water and sand inrush through mining-induced fractures in shallow bedrock under high water pressure. The model was simplified based on the engineering geology and hydrogeology of the thin-bedrock area of the Zhaogu Mine. Assuming that the hydraulic conductivity of the overlying aquifer was 0.43 m/days and a fracture, 20–30 cm wide and 5–15 m long, was formed in the roof after the inrush occurred, the diameter of the induced cone of depression in the aquifer would be at least 120 m. Considering the ease of operation and the size of the collected rock samples, a geometric similarity ratio of 200 was adopted in the test apparatus design. Gravity similarity was satisfied, based on the similarity theory of fluid mechanics, by matching the Froude number of the scaled model to that of the real situation.

### Rock Samples and the Test Apparatus

Rock samples were collected from shallow bedrock near face 11071 and were processed into cylinders (50 mm in height and 60 mm in diameter). A transparent cylindrical container was used to hold the samples, and the diameter of the container was designed as 70 mm, considering sealability and sample size (Fig. 7). A fracture 0.2 mm wide and 40 mm long was artificially created by splitting the cylindrical rock sample into two even parts along its axis and putting them

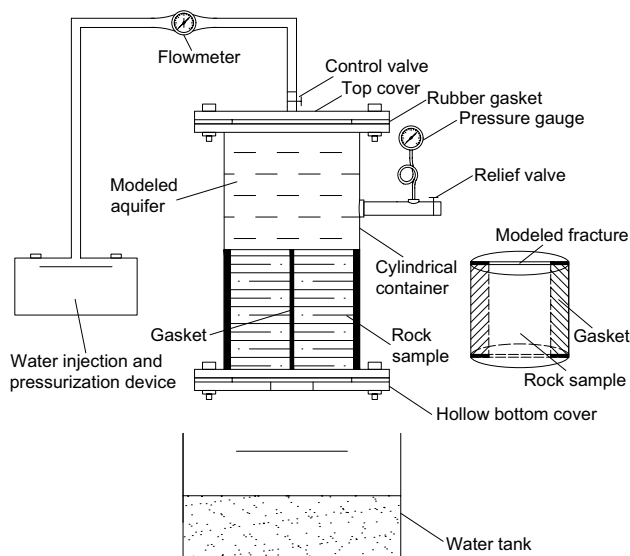


**Fig. 7** Apparatus for studying the failure process in mudstone under high water pressure

together with two gaskets in between (Fig. 7). Thus, the fracture penetrated the rock sample along the axial direction. To prevent water leakage from the junction, the gaskets were affixed with glass glue. A confined aquifer was modeled by attaching a water injection and pressurization device to the top of the cylindrical container. The bottom of the container was covered by a plate with a round opening in the middle, which allowed the water to flow into the water tank. The flow rates and water pressure, as key parameters affecting the failure process in mudstone, were measured in real time by a flowmeter and a pressure gauge.

### Test Scheme and Result Analysis

To observe fracture evolution in the mudstone under different water pressures, the water injection pressure was initially set at 0.1 MPa (Fig. 8a). Water flowed through the fracture and seeped through the fracture surface under pressure. The minerals in the mudstone expanded in volume as they became wet, resulting in gradual fracture closure. During the closure, a small amount of water discharge was first observed at the bottom of the container as the water pressure dropped below 0.1 MPa. The discharge soon transitioned into water drops before the fracture was finally blocked, and the water pressure gradually increased to its initial value (Phase I in Fig. 8). The water pressure was set to 0.15 MPa after 22 min. Seepage occurred through weak surfaces in

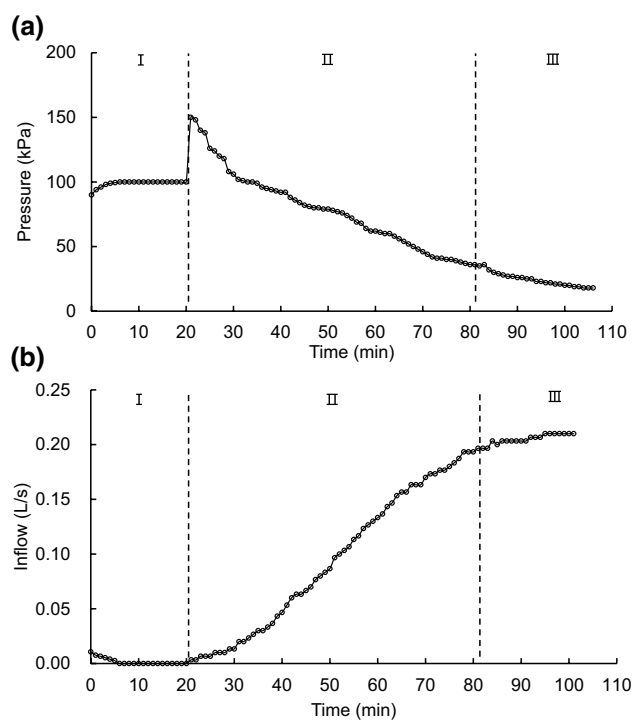


**Fig. 8** Changes of **a** water pressure in the modeled aquifer and **b** inflow from the modeled fracture reacting to different water pressures

the mudstone sample, and 2 min later, the water discharge was observed to increase as the water pressure significantly dropped (Phase II in Fig. 8). As the fracture was gradually eroded by the flowing water, the water pressure kept decreasing at a slower rate (Phase III in Fig. 8), and the fracture finally evolved into a 14 mm diameter cavity (Fig. 9).

The test results showed that the mudstone in the shallow bedrock had good water resistance under low water pressure. The induced fractures gradually close as the damp clays expand in volume. However, at higher water pressure, the mudstone weakens and the fractures enlarge. Based on analysis of the geological and hydrogeological conditions and the results of the geotechnical tests on the overlying strata, the mechanism of water and sand inrush that occurred at working face 11071 was concluded to be as follows: The impervious clay layers on top of and beneath the lowermost unconsolidated aquifer prevented water discharge to adjacent working faces, thus leading to higher water pressure in the aquifer. When mining occurred below the skylight area, mining-induced fractures developed upward into the confined aquifer. Water soon flowed into the fractures and disintegrated the mudstone. Though the mudstone minerals expanded in volume, the fractures were gradually eroded by the water and sand flowing at high water pressure. The inrush occurred when a large amount of water and sand from the aquifer gushed into the working face through these fractures.

### Modifications to the Design of Coal and Rock Pillars and Its Application

#### Modifications to the Design of the Coal and Rock Pillars

According to pillar categorization and design regulations in China (State Bureau of Coal Industry 2000), the protective coal and rock pillars of working face 11071 were categorized as sand-prevention pillars, and the pillars' minimum height had to exceed the sum of the maximum height of the caving zone and the height of a protective layer, as shown in Eq. (1):

$$H_s \geq H_m + H_b \tag{1}$$

where  $H_s$  is the minimum height of the sand-prevention coal and rock pillars,  $H_m$  is the maximum height of the caving zone, and  $H_b$  is the thickness of the protective layer, all in m.

The occurrence of the water and sand inrush at working face 11071 suggested the inapplicability of Eq. (1) for estimating the size of coal and rock pillars. Hence, equation modification was required to ensure mine safety. The physical simulation tests indicated that strongly weathered bedrock is likely to lose its resistance to sand and water below the skylight areas, given the negative effects of high water

pressure. To obtain the required resistance of the retained pillars, the thickness of the strongly weathered bedrock was included as an extra term,  $H_p$ , in Eq. (1):

$$H_s \geq H_m + H_b + H_p \tag{2}$$

where  $H_p$  is the protective thickness in the weathered zone under high water pressure, m. The value of  $H_p$  has to be decided based on the weathering extent of the shallow bedrock, per the example below.

### Engineering Application for Faces with Similar Geological Conditions

Face 11191 was located in the eastern coalfield of the Zhaogu Mine (see Figs. 1, 2) and had similar geological and mining conditions to face 11071. During the preparation stage, more than 30 drilling sites were constructed every 100 m along the headgate and the tailgate of face 11191. At each drilling site, several exploration boreholes were drilled in the roof to get the lithological characteristics and water abundance of the overlying strata. Different amounts of flowing sand, ranging from 0.5 to 5 m<sup>3</sup>, were found from the boreholes in the west where the bedrock was between 34.8 and 39.0 m thick and in the east where it was between 46.1 and 49.3 m thick (Fig. 2a).

Equation (2) was applied to the design of the sand-prevention coal and rock pillars at face 11191. The maximum height of the caving zone ( $H_m$ ) and the thickness of the protective layer ( $H_b$ ) were calculated considering the large mining height for the first slice ( $M=3.5$  m) and the moderately hard overlying strata (Xu and Liu 2011):

$$H_m = \frac{100M}{0.49M + 19.12} + 4.71 = 21.51 \text{ m}; H_b = 2.1M = 7.35 \text{ m}$$

The weathering extent of the shallow bedrock of working face 11191 was obtained using point load tests. Since the point load strength index of the rock samples from the roof of face 11191 was 0 in the first 5 m under the unconsolidated layers (see Group B in Fig. 5), the bedrock in this area was strongly weathered and its sand and water resistance might be weak under high water pressure. Thus, the protective thickness in the weathered zone under high water pressure ( $H_p$ ) was determined to be 5 m, and the minimum height of the sand-prevention coal and rock pillars was calculated:

$$H_s \geq H_m + H_b + H_p = 21.52 \text{ m} + 7.35 \text{ m} + 5 \text{ m} = 33.86 \text{ m}$$

Given that the mining height was 3.5 m, the height of the sand-prevention coal and rock pillars was set at 34 m. The thickness of the bedrock in the potential water and sand inrush areas was all greater than 34.8 m, and hence, the requirement was met for the height of the sand-prevention coal and rock pillars. Working face 11191 was safely mined,



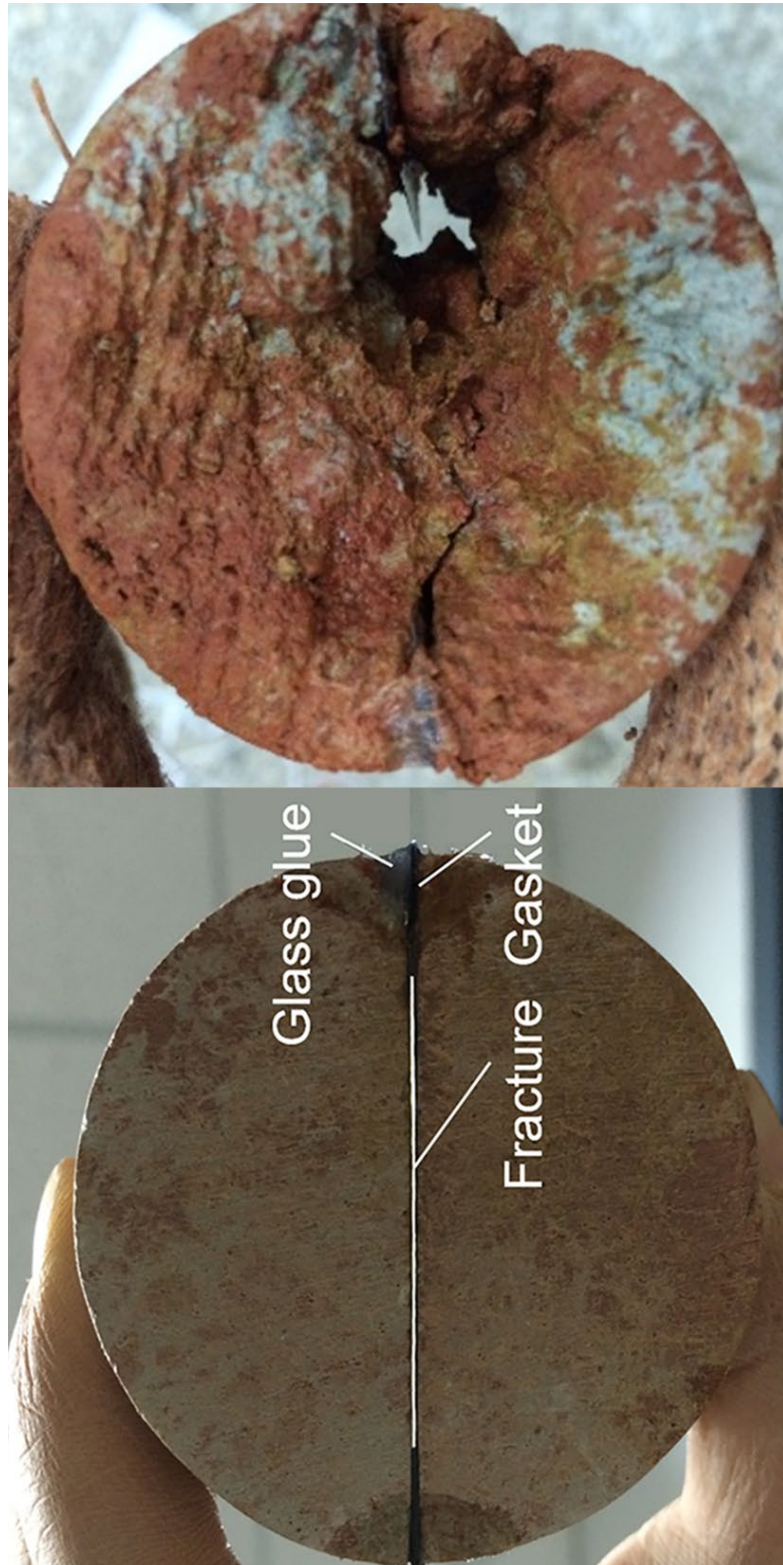


**Fig. 9** Comparison of the rock sample before (left) and after (right) the physical simulation tests

which shows the applicability of the modified equation when mining under a skylight area.

## Conclusions

Clay layers at the bottom of thick, unconsolidated layers in northern China help prevent water in overlying sand and gravel aquifers from flowing into working faces in shallow bedrock but can lead to high water pressure in the aquifers. Though weathered mudstone in the shallow bedrock is greatly weakened in strength, it also helps prevent water and sand inrush in the underlying faces as damp clay minerals expand in volume and block the flow paths. However, the clay layer will lose its water resistance once the water pressure exceeds a certain threshold. Under skylight areas, defined as places where horizontal confined aquifers extend and intersect inclined bedrock surfaces, mining-induced fractures in the shallow bedrock might be gradually eroded by water and sand flowing under high water pressure, potentially leading to inrush accidents at the working faces. In this case, the empirical formula for calculating sand-prevention coal and rock pillars needs to be modified by incorporating an extra term for protective thickness, which can be determined by the weathering extent of the shallow bedrock.

## References

- Bai M, Elsworth D (1990) Some aspects of mining under aquifers in China. *Min Sci Tech* 10:81–91
- Chen LW, Zhang SL, Gui HR (2014) Prevention of water and quicksand inrush during extracting contiguous coal seams under the lowermost aquifer in the unconsolidated Cenozoic alluvium—a case study. *Arab J Geosci* 7(6):2139–2149
- Chen LW, Feng XQ, Xie WP, Zeng W, Zheng ZY (2017) Using a fluid-solid coupled numerical simulation to determine a suitable size for barrier pillars when mining shallow coal seams beneath an unconsolidated, confined aquifer. *Mine Water Environ* 36(1):67–77
- Huang QX, Wei BN, Zhang WZ (2010) Study of downward crack closing of clay aquiclude in shallowly buried coal seam. *J Min Saf Eng* 27(1):35–39 (Chinese)
- Liu XS, Tan YL, Ning JG, Tian C, Wang J (2015) The height of water conducting fractured zones in longwall mining of shallow coal seams. *Geotech Geol Eng* 33:693–700
- Miao XX, Cui XM, Wang JA, Xu JL (2011) The height of fractured water-conducting zone in undermined rock strata. *Eng Geol* 120:32–39
- Qu YX, Xu XL, Shi MX, Wu ZL (1988) Engineering classification and fast estimation of the swelling potential for argillaceous rocks. *Hydrogeol Eng Geol* (5):13–16 (in Chinese)
- Shi WH, Yang TH, Yu QL, Li Y, Liu HL, Zhao YC (2017) A study of water-inrush mechanisms based on geo-mechanical analysis and an in-situ groundwater investigation in the Zhongguan iron mine, China. *Mine Water Environ* 36(3):409–417
- State Administration of Work Safety (2009) Provisions on prevention and control of water in coal mines. China Coal Industry Publ House, Beijing (in Chinese)
- State Bureau of Coal Industry (2000) Pillar design and mining regulations under buildings, water, rails and major roadways. China Coal Industry Publ House, Beijing (in Chinese)
- Sun YJ, Xu ZM, Dong QH, Liu SD, Gao RB, Jiang YH (2008) Forecasting water disaster for a coal mine under the Xiaolangdi reservoir. *J China Univ Min Technol* 18(4):516–520
- Tan YL, Liu XS, Ning JG, Lu YW (2017) In situ investigations on failure evolution of overlying strata induced by mining multiple coal seams. *Geotech Test J* 40(2):244–257
- Wang XZ, Xu JL, Zhu WB, Li YC (2012) Roof pre-blasting to prevent support crushing and water-inrush accidents. *Int J Min Sci Technol* 22(3):379–384
- Wu Q, Liu YZ, Zhou WF, Li BY, Zhao B, Liu SQ, Sun WJ, Zeng YF (2015) Evaluation of water inrush vulnerability from aquifers overlying coal seams in the Menkeqing Coal Mine, China. *Mine Water Environ* 34(3):258–269
- Xu YC (2008) Fluidity test on sand blended with clay. *J China Coal Soc* 33(5):496–499 (Chinese)
- Xu YC, Liu SQ (2011) Study on method to set safety coal and rock pillar for fully mechanized top coal caving mining under water body. *Coal Sci Technol* 39(11):1–4 (Chinese)
- Xu JL, Zhu WB, Wang XZ (2011) Study on water-inrush mechanism and prevention during coal mining under unconsolidated confined aquifer. *J Min Saf Eng* 28(3):333–339 (Chinese)
- Yang WF, Xia XH, Zhao GR, Ji YB, Shen DY (2011) Overburden failure and the prevention of water and sand inrush during coal mining under thin bedrock. *Min Sci Technol (China)* 21(5):733–736
- Yao BH, Bai HB, Zhang BY (2012) Numerical simulation on the risk of roof water inrush in Wuyang Coal Mine. *Int J Min Sci Technol* 22(2):273–277
- Zhang JC, Peng SP (2005) Water-inrush and environmental impact of shallow seam mining. *Eng Geol* 48(8):1068–1076
- Zhang JC, Shen BH (2004) Coal mining under aquifers in China: a case study. *Int J Rock Mech Min* 41(4):629–639
- Zhang HQ, He YN, Tang CA, Ahmad B, Han LJ (2009) Application of an improved flow-stress-damage model to the criticality assessment of water-inrush in a mine: a case study. *Rock Mech Rock Eng* 42(6):911–930
- Zhang DS, Fan GW, Ma LQ, Wang XF (2011) Aquifer protection during longwall mining of shallow coal seams: a case study in the Shendong Coalfield of China. *Int J Coal Geol* 86:90–196
- Zhang W, Shang YJ, Qu YX, Sun YC, Lin DM, Wang KY (2013a) Grain size distribution of collapsed scraps of argillaceous rock and its relationship with expansibility: an experimental study. *Rock Soil Mech* 34(1):66–72 (Chinese)
- Zhang YX, Tu SH, Bai QS, Li JJ (2013b) Overburden fracture evolution laws and water-controlling technologies in mining very thick coal seam under water-rich roof. *Int J Min Sci Technol* 23(5):693–700
- Zhang GM, Zhang K, Wang LJ, Wu Y (2015) Mechanism of water inrush and quicksand movement induced by a borehole and measures for prevention and remediation. *B Eng Geol Environ* 74(4):1395–1405
- Zhang GB, Zhang WQ, Wand CH, Zhu GL, Li B (2016) Mining thick coal seams under thin bedrock—deformation and failure of overlying strata and alluvium. *Geotech Geol Eng* 34(5):1553–1563
- Zhang WQ, Li B, Zhang GB, Li ZL (2017) Investigation of water-flow fracture zone height in fully mechanized cave mining beneath thick alluvium. *Geotech Geol Eng* 35(4):1745–1753
- Zhou DW, Wu K, Li L, Yu JW (2016) Impact of thick alluvial soil on a fractured water-conducting zone: an example from Huainan coal mine, China. *J S Afr I Min Metall* 116(5):431–440